**ISSN: 0067-2904**

# Stability analysis of the depletion of dissolved oxygen for the Phytoplankton-Zooplankton model in an aquatic environment

**Ahmed Ali, Shireen Jawad***
*Department of Mathematics, College of Science, University of Baghdad, Baghdad, Iraq*

Received: 6/4/2023 Accepted: 18/5/2023 Published: 30/5/2024

**Abstract**

Dissolved oxygen, phytoplankton, and zooplankton populations represent the basis of the proposed mathematical model designed to investigate the impact of the depletion of dissolved oxygen in the plankton ecosystem. The dynamic analysis of the model is devoted to locating all possible equilibrium points. The analysis demonstrates that three equilibrium positions are possible. The existence of the Hopf-bifurcation for the interior equilibrium is investigated using the phytoplankton's photosynthesis-produced oxygen rate as the bifurcation parameter. Conditions for stable limit cycles are obtained. In conclusion, a numerical simulation is shown as evidence to support the analytic results.

**Keywords**: Food chain model, Prey-predator model, Mutual interaction, Harvesting, Stability.

# تحليل استقرار استنفاد الأوكسجين المذاب لنموذج العوالق النباتية و الحيوانية في بيئة مائية

**أحمد علي احمد، شيرين رسول جواد***
قسم الرياضيات ، كلية العلوم ،جامعة بغداد ، قسم الرياضيات ، بغداد، العراق

**الخلاصة**

تشكل الأوكسجين المذاب و مجموعات العوالق النباتية و الحيوانية أساس النموذج الرياضي المقترح للتحقق من تأثير استنفاد الأوكسجين المذاب في النظام البيئي للعوالق. التحليل الديناميكي للنموذج مكرس لتحديد نقاط التوازن الممكنة. يوضح التحليل أن ثلاثة أوضاع توازن ممكنة. تم التحقق من وجود تشعب هوبف للتوازن الداخلي باستخدام معدل الأوكسجين الناتج عن التمثيل الضوئي للعوالق النباتية كمعامل التشعب. يتم الحصول على شروط دورات الحد المستقرة. في الختام ، يتم عرض محاكاة عددية كدليل لدعم النتائج التحليلية.

## 1. Introduction

Since dissolved oxygen dynamics are such an important indication of the overall health of marine ecosystems. There is a lot of interest in trying to understand them better [1-3]. Phytoplankton is the most plant-like planktonic communities; they produce most of the oxygen in the seas through photosynthesis that represents the basis of the marine food web. It is well-known that changes in factors like salinity, temperature, and nutrient availability greatly affect the quantity of oxygen phytoplankton production. In addition, phytoplankton's

* Email: shireenjawad82@gmail.com

oxygen production varies significantly between day and night. Therefore, the relationship between phytoplankton and dissolved oxygen is vital to the survival of most species from the simplest (a single cell) to the most complex. Changes in the production of oxygen can have profound effects on marine life [4]. Some environmental factors, such as temperature, influence the proliferation and biomass of phytoplankton. Oxygen is produced during photosynthesis during the day and absorbed during respiration at night, so dissolved oxygen levels in water fluctuate daily. Therefore, phytoplankton communities are useful indicators of environmental changes [5-7]. There are many studies on this important issue, for instance, Mondal et al. [8] studied the coupled plankton-oxygen dynamics in the ocean that are affected by a low oxygen production rate which can result in oxygen depletion and species extinction. Furthermore, the primary objective of the study of theoretical ecology is to identify the various dynamical mechanisms underlying interactions between prey and predator [9-15]. The relationship between phytoplankton and zooplankton is an example of a predator-prey interaction that reveals numerous aspects of marine ecology. Phytoplankton contributes substantially to aquatic ecosystems including producing vast quantities of oxygen, managing natural resources and water quality that can establish numerous food webs [16]. Plankton dynamics research is a fascinating field of study. Plankton constitutes the building elements of all aquatic food chains with phytoplankton occupying the first trophic level [17]. Toxins are produced by phytoplankton which serves an essential environmental function and cannot be ignored. It has been demonstrated that environmental stress factors, optimal environmental conditions, nutrient-limited environments, and others. Similar factors are significant contributors to the release of pollutants. Certain phytoplankton species are notorious for generating and emitting toxic or allelochemicals which can be detrimental to other phytoplankton species [18]. For instance, Venturino et al. [19] demonstrated that toxin-producing phytoplankton acts as a control agent for the cessation of plankton blooms. Baghel and Dhar [20] examined the effect of dissolved oxygen on the presence of a planktonic population that interacts. They conclude that the Hopf-bifurcation in the interior equilibrium is possible if the phytoplankton growth rate is selected as the bifurcation parameter.

This study aims to investigate the oxygen-plankton model's dynamics due to the combined effects of the phytoplankton refuge and the toxins produced by phytoplankton. In addition, we assume that the zooplankton consumes both hazardous and non-toxic phytoplankton in our model. We also consider that certain phytoplankton species can avoid zooplankton predators by hiding in different bottom strata. These sediments provide a cover for the prey from their predators. The structure of this work is as follows: In Section 2, we build the structure of the proposed model. Section 3 explains the feasibility requirements and stability conditions for all steady states. The prevalence of the Hopf bifurcations is also illustrated in Section 4. In Section 5, we undertake the MATLAB program for the numerical simulations to validate the analytical results.

## 2. Assumptions of the Model

Let $u(t)$ be the phytoplankton population at time $t$; phytoplankton is expected to come in two kinds, toxic and non-toxic. $v(t)$ is the zooplankton density at time $t$; assuming that zooplankton feeds on the preceding two categories. In addition, we believe that some phytoplankton populations have a low risk of being consumed by zooplankton if they can hide in the various sediments found on the seafloor. These sediments provide a cover for the prey from their predators. $w(t)$ represents the dissolved oxygen concentration in an aquatic environment. The phytoplankton also releases oxygen into the atmosphere since they carry out photosynthesis throughout the day. The pace of oxygen depletion is also influenced by several other variables including the breathing of marine creatures, the use of oxygen by phytoplankton at night, and the progressive decrease in oxygen concentration brought on by

chemical processes in the water. The following set of ordinary differential equations governs the structure of the dynamics of the proposed system:

$$\begin{aligned}\frac{du}{dt} &= \frac{ru}{(a_1 + w_0 - w)} - \alpha_1 u(1-m)v - \delta_1 u = f_1(u,v,w),\\ \frac{dv}{dt} &= \frac{\alpha_2 u(1-m)v}{(a_2 + w_0 - w)} - \delta_2 v - au(1-m)v = f_2(u,v,w),\\ \frac{dw}{dt} &= s(w_0 - w) + du - \gamma w - \gamma_1 uw - \gamma_2 vw = f_3(u,v,w).\end{aligned} \tag{1}$$

with the initial conditions $u(0) = u_{00} \geq 0, v(0) = v_{00} \geq 0$ and $w(0) = w_{00} \geq 0$. In the first equation of the system (1), $\frac{ru}{(a_1+w_0-w)}$ represents the absorption of dissolved oxygen from phytoplankton with the growth rate $r$. The maximum growth rate of the phytoplankton population is $r/a_1$ at $w = w_0$. Moreover, $(1-m)$ represents the proportion of unprotected toxic and non-toxic phytoplankton consumed by various zooplankton types. All parameters for the dissolved oxygen-phytoplankton-zooplankton model are assumed to be positive. The description of the system (1) parameters is clarified in Table 1.

**Table 1:** System's (1) Parameters description.

| Parameters | Biological interpretation |
|---|---|
| $r$ | The growth rate of phytoplankton. |
| $\alpha_1$ | The capture rate of the available non-toxic phytoplankton by zooplankton. |
| $m \in (0,1)$ | The proportion of protected phytoplankton. |
| $\alpha_2$ | The conversion rate from phytoplankton to zooplankton. |
| $a$ | The predation rate of toxic phytoplankton by zooplankton. |
| $\delta_1$ | The phytoplankton's natural death rate. |
| $\delta_2$ | The zooplankton's natural death rate. |
| $a_1$ | The phytoplankton saturation constant. |
| $a_2$ | the zooplankton saturation constant. |
| $w_0$ | The constant concentration of dissolved oxygen that comes from other sources. |
| $s$ | The replenishment rate of oxygen in marine. |
| $d$ | the amount of oxygen produced as a result of the process of photosynthesis carried out by phytoplankton. |
| $\gamma$ | the natural depletion rate of oxygen. |
| $\gamma_1$ | The consumption of oxygen by phytoplankton during the night. |
| $\gamma_2$ | The consumption of oxygen by zooplankton. |

Further, the following Figure illustrates the schematic sketch of the system (1).

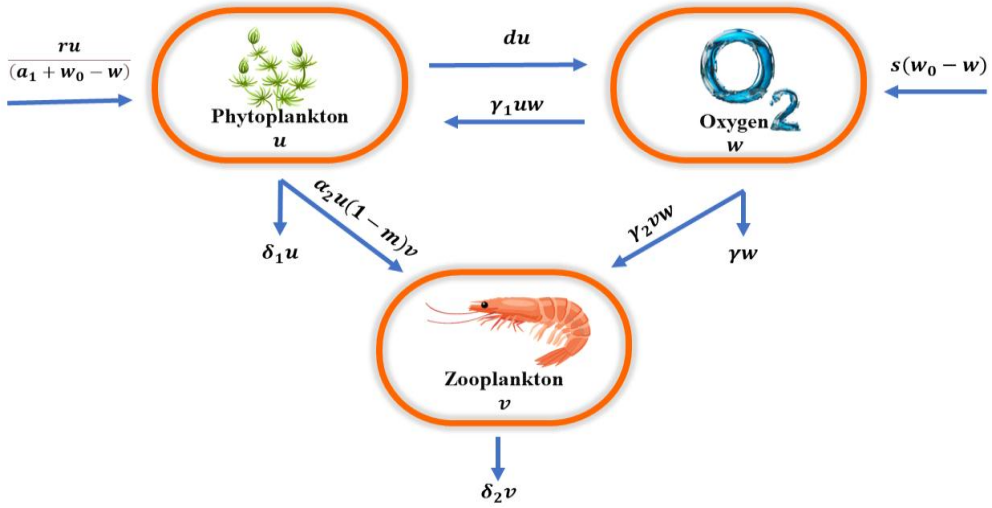


**Figure 1:** Schematic diagram of the system (1).

In addition, the right-hand side equations of the system (1) are $C^1(R_+^3)$, where $R_+^3 = \{(u,v,w), u \geq 0, v \geq 0,\ w \geq 0\}$. Consequently, they are Lipschitzian. Therefore, the solution of the system (1) exists and is unique.

## 3. Existence of equilibria

System (1) has three non-negative steady points, namely:

1. The dissolved oxygen equilibrium point (DOEP) is given by $F_1 = (0,0,\widehat{w})$, where $\widehat{w} = \frac{sw_0}{s+\gamma}$.

2. The zooplankton free equilibrium point (ZFEP) is given by $F_2 = (\bar{u}, 0, \bar{w})$, where $\bar{w} = a_1 + w_0 - \frac{r}{\delta_1}$, and $\bar{u} = \frac{(s+\gamma)}{d-\gamma_1\left(a_1+w_0-\frac{r}{\delta_1}\right)}\left[a_1 - \frac{r}{\delta_1}\right]$. For $\bar{u}$ and $\bar{w}$ to be positive, the following two conditions must be satisfied:

$$a_1 + w_0 - \frac{d}{\gamma_1} < \frac{r}{\delta_1} < a_1. \quad (1)$$

3. The coexisting equilibrium point (CEP) given by $F_3 = (u^*, v^*, w^*)$, where $u = \frac{\delta_2(a_2+w_0-w)}{(1-m)[\alpha_2-a(a_2+w_0-w)]}$, $v = \frac{r}{\alpha_1(1-m)(a_1+w_0-w)} - \frac{\delta_1}{\alpha_1(1-m)}$, and $w$ is the root of the following equation:

$$B_0 w^3 + B_1 w^2 + B_2 w + B_3 = 0, \quad (3)$$

where

$B_0 = a\alpha_1(1-m)(s+\gamma) > 0,$

$B_1 = \alpha_1 asw_0[2-(1-m)] + d\delta_2\alpha_1 - \alpha_1(s+\gamma)(\alpha_2 - aa_2) - \alpha_1 a\gamma[a_1(1-m) - 2w_0],$

$B_2 = \alpha_1 asw_0(1-m)(2a_1+3w_0) - \alpha_1 w_0(1-m)(s+\gamma)[\alpha_2 - aa_2] - d\delta_2\alpha_1 a_1 +$
$\alpha_1(1-m)(s+\gamma)[aa_1a_2 - \alpha_2 a_1 + aw_0^2] + \alpha_1 a\gamma w_0(1-m)(a_1+w_0),$

$B_3 = \alpha_1 sw_0(1-m)[\alpha_2 a_1 - aa_1a_2 - aa_1w_0 + \alpha_2 w_0 - a\alpha_2 w_0 - aw_0^2] + d\delta_2\alpha_1[a_1a_2 +$
$a_1w_0 + a_2w_0 + w_0^2].$

Using Descartes's rule of sign, equation (3) has a unique positive root, say $w = w^*$, if one of the following sets of conditions hold:

$$B_1 > 0 \text{ and } B_3 < 0, \quad (4)$$

$$B_2 < 0 \text{ and } B_3 < 0. \quad (5)$$

For $u^*$and $v^*$to be positive, the following two conditions must be satisfied:

$$\alpha_2 > a(a_2 + w_0 - w), \quad (6)$$

$$r > \delta_1(a_1 + w_0 - w). \quad (7)$$

## 4. The stability analysis

The feature of the eigenvalues of the Jacobian matrix $J(u,v,w)$ at an equilibrium point is directly related to the behavior of the system (1) near an equilibrium point. The $J(u,v,w)$ at any point, say $(u,v,w)$, can be written as follows:

$$J = \left(a_{ij}\right)_{3\times 3},$$

where $a_{11} = \frac{r}{(a_1+w_0-w)} - \alpha_1 v(1-m) - \delta_1 \quad a_{12} = -\alpha_1(1-m)u; \quad a_{13} = \frac{ru}{(a_1+w_0-w)^2};$
$a_{21} = \frac{\alpha_2(1-m)v}{(a_2+w_0-w)} - a(1-m)v; \quad a_{22} = \frac{\alpha_2(1-m)u}{(a_2+w_0-w)} - \delta_2 - a(1-m)u; \quad a_{23} = \frac{\alpha_2 u(1-m)v}{(a_2+w_0-w)^2};$
$a_{31} = d - \gamma_1 w;\ a_{32} = -\gamma_2 w;\ a_{33} = -(s+\gamma+\gamma_1 u+\gamma_2 v).$

Keeping this in mind, we take a look at the system (1) around each equilibrium point:

**1.** The Jacobian matrix at the $F_1 = (0,0,\widehat{w})$ is given as:

$$J(F_1) = \begin{bmatrix} \frac{r}{(a_1+w_0-\widehat{w})} - \delta_1 & 0 & 0 \\ 0 & -\delta_2 & 0 \\ d-\gamma_1\widehat{w} & -\gamma_2\widehat{w} & -s-\gamma \end{bmatrix}$$

Then, $J(F_1)$ has the eigenvalues $\lambda_{11} = \frac{r}{(a_1+w_0-\widehat{w})} - \delta_1$, $\lambda_{12} = -\delta_2 < 0$, and $\lambda_{13} = -s-\gamma$. $F_1$ is a locally asymptotically stable point if and only if

$$r < \delta_1(a_1+w_0-\widehat{w}). \tag{8}$$

**2.** The Jacobian matrix at the $F_2 = (\bar{u},0,\bar{w})$ is given as:

$$J(F_2) = \begin{bmatrix} \frac{r}{(a_1+w_0-\bar{w})} - \delta_1 & -\alpha_1\bar{u}(1-m) & \frac{r\bar{u}}{(a_1+w_0-\bar{w})^2} \\ 0 & \frac{\alpha_2\bar{u}(1-m)}{(a_2+w_0-\bar{w})} - \delta_2 - a\bar{u}(1-m) & 0 \\ d-\gamma_1\bar{w} & -\gamma_2\bar{w} & -s-\gamma-\gamma_1\bar{u} \end{bmatrix}.$$

Then, the characteristic equation of $J(F_2)$ is given by:

$$\left(\frac{\alpha_2\bar{u}(1-m)}{(a_2+w_0-\bar{w})} - \delta_2 - a\bar{u}(1-m) - \lambda\right)\left[\lambda^2 - Tr\big(J(F_2)\big)\lambda + Det\big(J(F_2)\big)\right]$$

The eigenvalues of the above equation can be written as follows

$\lambda_{21} = \frac{\alpha_2\bar{u}(1-m)}{(a_2+w_0-\bar{w})} - \delta_2 - a\bar{u}(1-m),$

$Tr\big(J(F_2)\big) = \frac{r}{(a_1+w_0-\bar{w})} - \delta_1 - (s+\gamma+\gamma_1\bar{u}),$

$Det\big(J(F_2)\big) = \delta_1(s+\gamma+\gamma_1\bar{u}) - \frac{r(s+\gamma+\gamma_1\bar{u})}{(a_1+w_0-\bar{w})} + \frac{r\bar{u}\ (\gamma_1\bar{w}-d)}{(a_1+w_0-\bar{w})^2}.$

Clearly, $F_2$ is a locally asymptotical stable point if and only if the following conditions are satisfied:

$$\delta_2 + a\bar{u}(1-m) > \frac{\alpha_2\bar{u}(1-m)}{(a_2+w_0-\bar{w})}. \tag{9.1}$$

$$r < [\delta_2 + (s+\gamma+\gamma_1\bar{u})](a_1+w_0-\bar{w}), \tag{9.2}$$

$$\delta_1(s+\gamma+\gamma_1\bar{u}) + \frac{r\bar{u}\ (\gamma_1\bar{w}-d)}{(a_1+w_0-\bar{w})^2} > \frac{r(s+\gamma+\gamma_1\bar{u})}{(a_1+w_0-\bar{w})}. \tag{9.3}$$

**3.** The Jacobian matrix at the CEP $F_3 = (u^*,v^*,w^*)$ is given as:

$$J(F_3) = \begin{bmatrix} a_{11}^{[3]} & a_{12}^{[3]} & a_{13}^{[3]} \\ a_{21}^{[3]} & a_{22}^{[3]} & a_{23}^{[3]} \\ a_{31}^{[3]} & a_{32}^{[3]} & a_{33}^{[3]} \end{bmatrix}, \tag{10}$$

where, $a_{11}^{[3]} = \frac{r}{(a_1+w_0-w^*)} - \delta_1 - \alpha_1 v^*(1-m)$; $a_{12}^{[3]} = -\alpha_1 u^*(1-m)$; $a_{13}^{[3]} = \frac{ru^*}{(a_1+w_0-w^*)^2}$; $a_{21}^{[3]} = \frac{\alpha_2 v^*(1-m)}{(a_2+w_0-w^*)} - av^*(1-m)$; $a_{22}^{[3]} = 0$, $a_{23}^{[3]} = \frac{\alpha_2 u^*(1-m)v^*}{(a_2+w_0-w^*)^2}$,; $a_{31}^{[3]} = d-\gamma_1 w^*$; $a_{32}^{[3]} = -\gamma_2 w^*$; $a_{33}^{[3]} = -s-\gamma-\gamma_1 u^*-\gamma_2 v^*$.

So, the characteristic equation of $J(F_3)$ can be written as:

$$\lambda^3 + A_1\lambda^2 + A_2\lambda + A_3 = 0, \tag{11}$$

where

$A_1 = -\left(a_{11}^{[3]} + a_{33}^{[3]}\right)$,

$A_2 = -(a_{13}^{[3]}a_{31}^{[3]} + a_{23}^{[3]}a_{32}^{[3]} + a_{12}^{[3]}a_{21}^{[3]} - a_{11}^{[3]}a_{33}^{[3]})$,

$A_3 = a_{11}^{[3]}a_{23}^{[3]}a_{32}^{[3]} + a_{12}^{[3]}a_{21}^{[3]}a_{33}^{[3]} - a_{13}^{[3]}a_{21}^{[3]}a_{32}^{[3]} - a_{12}^{[3]}a_{23}^{[3]}a_{31}^{[3]}$,

$\Delta = A_1A_2 - A_3 = \left(a_{11}^{[3]} + a_{33}^{[3]}\right)\left(a_{13}^{[3]}a_{31}^{[3]} - a_{11}^{[3]}a_{33}^{[3]}\right) + a_{11}^{[3]}a_{12}^{[3]}a_{21}^{[3]} + a_{23}^{[3]}a_{32}^{[3]}a_{33}^{[3]} + a_{12}^{[3]}a_{23}^{[3]}a_{31}^{[3]} + a_{13}^{[3]}a_{21}^{[3]}a_{32}^{[3]}$.

Now, from the Routh-Hurwitz criteria, $F_3$ is a LAS point, under the following condition $A_1 > 0, A_3 > 0$ and $\Delta > 0$.

In the following theorem, adequate conditions for the global stability of the CEP which is given by $F_3 = (u^*, v^*, w^*)$ are identified by the Lyapunov method.

**Theorem 1.** Assume that

$$\left.\begin{array}{c}[(s+\gamma)+\gamma_1 u+\gamma_2 v](w-w^*) > [d+w^*](u-u^*)+w^*(v-v^*) \\ \alpha_2 > a\end{array}\right\}. \tag{12}$$

Then CEP is globally asymptotically stable in $R_+^3$.

**Proof:-** Define $G_3 = c_1\left(u-u^*-u^*\ln\frac{u}{u^*}\right) + c_2\left(v-v^*-v^*\ln\frac{v}{v^*}\right) + c_3\left(\frac{w-w^*}{2}\right)^2$, where $c_1$, $c_2$ and $c_3$ are positive constants to be specified and $G_3(u,v,w)$ is a positive definite function about CEP. Thus,

$$\frac{dG_3}{dt} = \frac{c_1(u-u^*)}{u}\frac{du}{dt} + \frac{c_2(v-v^*)}{v}\frac{dv}{dt} + c_3(w-w^*)\frac{dw}{dt}$$

By choosing the constants $c_2 = c_3 = 1$, $c_1 = \frac{(\alpha_2-a)}{\alpha_1}$, and using model (1) with some algebraic manipulations, we get:

$$\frac{dG_3}{dt} \le -[(s+\gamma)+\gamma_1 u+\gamma_2 v](w-w^*)^2 + [d+w^*](u-u^*)(w-w^*) + w^*(v-v^*)(w-w^*).$$

Then, $\frac{dG_3}{dt} < 0$ under condition (12). Hence, $G_3$ is a Lyapunov function. Therefore, CEP is globally asymptotically stable in $R_+^3$ if $u$, $v$ and $w$ are controlled by condition (12).

## 5. The Hopf bifurcation analysis

The Hopf bifurcation refers to the local birth or death of a periodic solution from equilibrium as a parameter crosses a critical value. In a differential equation, the Hopf bifurcation typically occurs when a complex conjugate pair of eigenvalues of the linearised flow at a fixed point becomes purely imaginary. Hopf bifurcation threshold and its conditions are clarified in the following theorem.

**Theorem 2:-** Under the following assumptions:

$$A_i > 0, i = 1, \tag{13.1}$$

$$a_{12}a_{23} - a_{13}A_1'(d^*) \neq 0, \tag{13.2}$$

$$d^* > 0, \tag{13.3}$$

where Ai's are the coefficients of the characteristic equation given in equation (11) with $d = d^*$ and the formula for $d^*$ is shown in the following proof. Then, there exists a Hopf bifurcation for CEP at $d = d^*$.

**Proof:-** The value of the bifurcation parameter can be found if we set $A_1(d^*)A_2(d^*) - A_3(d^*) = 0$ in equation (11). This gives:

$d^* = \frac{a_{11}(a_{33}-a_{12}a_{21}+a_{33}^2)-a_{23}(a_{32}a_{33}+a_{12}a_{31})+a_{13}a_{21}a_{32})}{(a_{11}+a_{33})a_{13}} + \gamma_1 w^*.$

Clearly, $d^* > 0$ if condition (13.3) holds. Now, at $d = d^*$, equation (11) can be written as

$$(\lambda + A_1)(\lambda^2 + A_2) = 0.$$

According to condition (13.1), the above equation has three roots, the negative root $\lambda_1 = -A_1$ and two purely imaginary roots $\lambda_{2,3} = \pm i\sqrt{A_2}$. In a neighborhood of $d^*$, the roots have the following forms: $\lambda_1 = -A_1, \lambda_{2,3} = \rho_1(d) \pm i\rho_2(d)$.

Clearly, $Re(\lambda_{2,3})|_{d=d^*} = \rho_1(d^*) = 0$ indicates that the first condition for the Hopf bifurcation has been met at $d = d^*$. Now to confirm the transversality condition, we substitute $\rho_1(d) \pm i\rho_2(d)$ into equation (11) and then compute its derivative with respect to $d^*$, $\Theta(d^*)\psi(d^*) + \Gamma(d^*)\phi(d^*) \neq 0$, where the form of $\Theta(d^*), \psi(d^*), \Gamma(d^*)$ and $\phi(d^*)$ are

$\psi(d) = 3\rho_1^2(d) + 2A_1(d)\rho_1(d) + A_2(d) - 3\rho_2^2(d),$
$\phi(d) = 6\rho_1(d)\rho_2(d) + 2A_1(d)\rho_2(\gamma_1),$
$\Theta(d) = \rho_1^2(d)A_1\,'(d) + A_2\,'(d)\rho_1(d) + A_3\,'(d) - A_1\,'(d)\rho_2^2(d),$
$\Gamma(d) = 2\rho_1(d)\rho_2(d)A_1'(d) + A_2'(d)\rho_2(d).$

Now at $d = d^*$, substitution $\rho_1 = 0$ and $\rho_2 = \sqrt{A_2}$, into equation (11), the following is obtained:

$$\psi(d^*) = -2A_2(d^*),$$
$$\phi(d^*) = 2A_1(d^*)\sqrt{A_2(d^*)},$$
$$\Theta(d^*) = A_3'(d^*) - A_1'(d^*)A_2(d^*),$$
$$\Gamma(d^*) = A_2'(d^*)\sqrt{A_2(d^*)},$$

where

$$A_1'(d^*) = 0,$$
$$A_2'(d^*) = a_{13},$$
$$A_3'(d^*) = -a_{12}a_{23}.$$

Hence, condition (12) gives

$$\Theta(d^*)\psi(d^*) + \Gamma(d^*)\phi(d^*) = -2A_2(d^*)[a_{12}a_{23} - a_{13}A_1'(d^*)] \neq 0.$$

That means the Hop bifurcation has occurred at $d = d^*$ then the proof is completed.

From Theorem 3, the stability condition of the stable limit cycle in $R_+^3$ is presented using the coefficient of curvature of the limit cycle. For a detailed discussion, we refer to [26].

**Theorem 3** The system (1) has a stable limit cycle in $R^3_{(u,v,w)}$ if the following condition is true:

$$\frac{r}{(a_1+w_0-u_3-w^*)^2} \neq \frac{\alpha_2(u_1+u^*)(1-m)}{(a_2+w_0-u_3-w^*)^2}. \quad (14)$$

**Proof:-** By using transformations $u = u_1 + u^*$, $v = u_2 + v^*$, $w = u_3 + w^*$, the CEP equilibrium point shifted to (0,0,0), and the system (1) becomes

$$\frac{du_1}{dt} = \frac{r(u_1 + u^*)}{(a_1 + w_0 - u_3 - w^*)} - \alpha_1(u_1 + u^*)(u_2 + v^*)(1 - m) - (u_1 + u^*)\delta_1$$
$$\frac{du_2}{dt} = \frac{\alpha_2(u_1 + u^*)(u_2 + v^*)(1 - m)}{(a_2 + w_0 - u_3 - w^*)} - \delta_2(u_2 + v^*) - a(u_1 + u^*)(u_2 + v^*)(1 - m)$$

$$\frac{du_3}{dt} = s[w_0 - (u_3 + w^*)] + d(u_1 + u^*) - \gamma(u_3 + w^*) - \gamma_1(u_1 + u^*)(u_3 + w^*) - \gamma_2(u_2 + v^*)(u_3 + w^*),$$

where the nonlinear part of the above system is presented in the following matrix is

$$\mho = \begin{pmatrix} \mho_1 \\ \mho_2 \\ \mho_3 \end{pmatrix} = \begin{pmatrix} \frac{r(u_1 + u^*)}{(a_1 + w_0 - u_3 - w^*)} - \alpha_1(1-m)u_1u_2 \\ \frac{\alpha_2(u_1 + u^*)(u_2 + v^*)(1-m)}{(a_2 + w_0 - u_3 - w^*)} - a(1-m)u_1u_2 \\ -\gamma_1 u_1 u_3 - \gamma_2 u_2 u_3 \end{pmatrix}$$

We derive the following characteristic quantities from the nonlinear part:

$g_{20}^0 = \frac{1}{4}\left\{\frac{\partial^2\mho_1}{\partial u_1^2} - \frac{\partial^2\mho_1}{\partial u_2^2} + 2\frac{\partial^2\mho_2}{\partial u_1 \partial u_2} + i\left(\frac{\partial^2\mho_2}{\partial u_1^2} - \frac{\partial^2\mho_2}{\partial u_2^2} - 2\frac{\partial^2\mho_1}{\partial u_1 \partial u_2}\right)\right\} = \frac{1}{2}\left\{\frac{\alpha_2(1-m)}{(a_2+w_0-u_3-w^*)} + \alpha_1(1-m)i\right\},$

$g_{11}^0 = \frac{1}{4}\left\{\frac{\partial^2\mho_1}{\partial u_1^2} + \frac{\partial^2\mho_1}{\partial u_2^2} + i\left(\frac{\partial^2\mho_2}{\partial u_1^2} + \frac{\partial^2\mho_2}{\partial u_2^2}\right)\right\} = 0,$

$G_{110}^0 = \frac{1}{2}\left\{\frac{\partial^2\mho_1}{\partial u_1 \partial u_3} + \frac{\partial^2\mho_2}{\partial u_2 \partial u_3} + i\left(\frac{\partial^2\mho_2}{\partial u_1 \partial u_3} - \frac{\partial^2\mho_1}{\partial u_2 \partial u_3}\right)\right\} = \frac{1}{2}\left\{\frac{r}{(a_1+w_0-u_3-w^*)^2} + \frac{\alpha_2(u_1+u^*)(1-m)}{(a_2+w_0-u_3-w^*)^2} + i\left(\frac{\alpha_2(u_2+v^*)(1-m)}{(a_2+w_0-u_3-w^*)^2}\right)\right\},$

$G_{101}^0 = \frac{1}{2}\left\{\frac{\partial^2\mho_1}{\partial u_1 \partial u_3} - \frac{\partial^2\mho_2}{\partial u_2 \partial u_3} + i\left(\frac{\partial^2\mho_2}{\partial u_1 \partial u_3} + \frac{\partial^2\mho_1}{\partial u_2 \partial u_3}\right)\right\} = \frac{1}{2}\left\{\frac{r}{(a_1+w_0-u_3-w^*)^2} - \frac{\alpha_2(u_1+u^*)(1-m)}{(a_2+w_0-u_3-w^*)^2} + i\left(\frac{\alpha_2(u_2+v^*)(1-m)}{(a_2+w_0-u_3-w^*)^2}\right)\right\},$

$W_{11}^0 = -\frac{1}{4\lambda_3(a_1(k^*)}\left(\frac{\partial^2\mho_3}{\partial u_1^2} + \frac{\partial^2\mho_3}{\partial u_2^2}\right) = 0,$

$W_{20}^0 = -\frac{1}{4\lambda_3(a_1(k^*)}\left(\frac{\partial^2\mho_3}{\partial u_1^2} + \frac{\partial^2\mho_3}{\partial u_2^2} - 2i\frac{\partial^2\mho_3}{\partial u_1 \partial u_2}\right) = 0,$

$G_{21}^0 = \frac{1}{8}\left\{\frac{\partial^3\mho_1}{\partial u_1^3} + \frac{\partial^3\mho_1}{\partial u_1 \partial u_2^2} + \frac{\partial^3\mho_2}{\partial u_2^3} + \frac{\partial^3\mho_2}{\partial u_1^2 \partial u_2} + i\left(\frac{\partial^3\mho_2}{\partial u_1^3} + \frac{\partial^3\mho_2}{\partial u_1 \partial u_2^2} - \frac{\partial^3\mho_1}{\partial u_2^3} - \frac{\partial^3\mho_1}{\partial u_1^2 \partial u_2}\right)\right\} = 0,$

Thus, the coefficient of the curvature of the limit cycle is given by

$\sigma_1^0 = Re\left\{\frac{g_{20}^0 g_{11}^0}{4} i + G_{110}^0 W_{11}^0 + \frac{G_{21}^0 + G_{101}^0 W_{20}^0}{2}\right\},$

$\sigma_1^0 = Re\frac{1}{4}\left\{\frac{r}{(a_1+w_0-u_3-w^*)^2} - \frac{\alpha_2(u_1+u^*)(1-m)}{(a_2+w_0-u_3-w^*)^2} + i\left(\frac{\alpha_2(u_2+v^*)(1-m)}{(a_2+w_0-u_3-w^*)^2}\right)\right\} = \frac{r}{(a_1+w_0-u_3-w^*)^2} - \frac{\alpha_2(u_1+u^*)(1-m)}{(a_2+w_0-u_3-w^*)^2}.$

Thus, condition (14) guarantees that system (1) has a stable limit cycle; the proof is completed.

## 6. Numerical analysis

To validate our theoretical conclusions and get insight into the many possible dynamics of the system (1), we conduct a numerical simulation here using MATLAB 2019b program to create all figures, while the numerical solution to our system was found using the ode45 solver. Our primary objective is to examine the dynamics of the depletion of dissolved oxygen for the phytoplankton-zooplankton interaction. For the specified variables:

$$\begin{aligned} &\mathrm{r} = 0.36, \alpha_1 = 0.25, \alpha_2 = 0.18,\ \delta_1 = 0.1, \delta_2 = 0.1, m = \\ &0.26, a_1 = 0.2, a_2 = 0.2, w_0 = 3, a = 0.02, s = 2.85, \gamma_1 = \\ &0.18, \gamma_2 = 0.2, \gamma = 0.2, d = 0.4, \end{aligned} \tag{15}$$

and with different initial values, it is observed from Figure (2) that $F_3 = (0.63, 2.12, 2.41)$ is a globally asymptotically stable point.

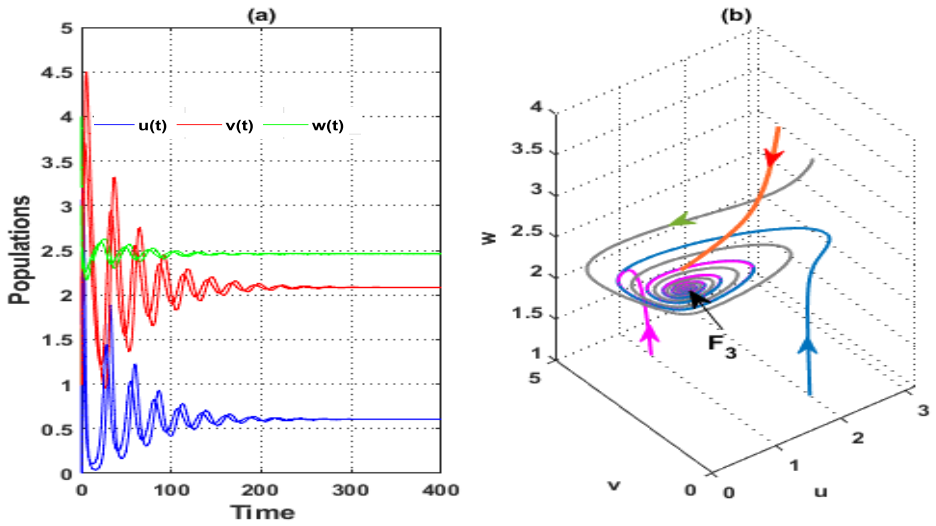


**Figure 2:** Phase diagram of system (1) with the data set given by (15) with different initial values.

To examine the effect of varying one parameter at a time on the behavior of system (1), it has been numerically resolved for the data in (15). In light of this, Figure (3) investigates the effect of change in the phytoplankton's growth rate $(r)$, on the stability behaviour of system (1). The simulation shows when $r \leq 0.1$, the system (1) has no CEP, and the solution settles down to DOEP, $F_1 = (0, 0, 2.81)$, in the $w$- axis. While for $r > 0.1$, the solution converges asymptotically to CEP, $F_3 = (0.85, 4.27, 2.19)$.

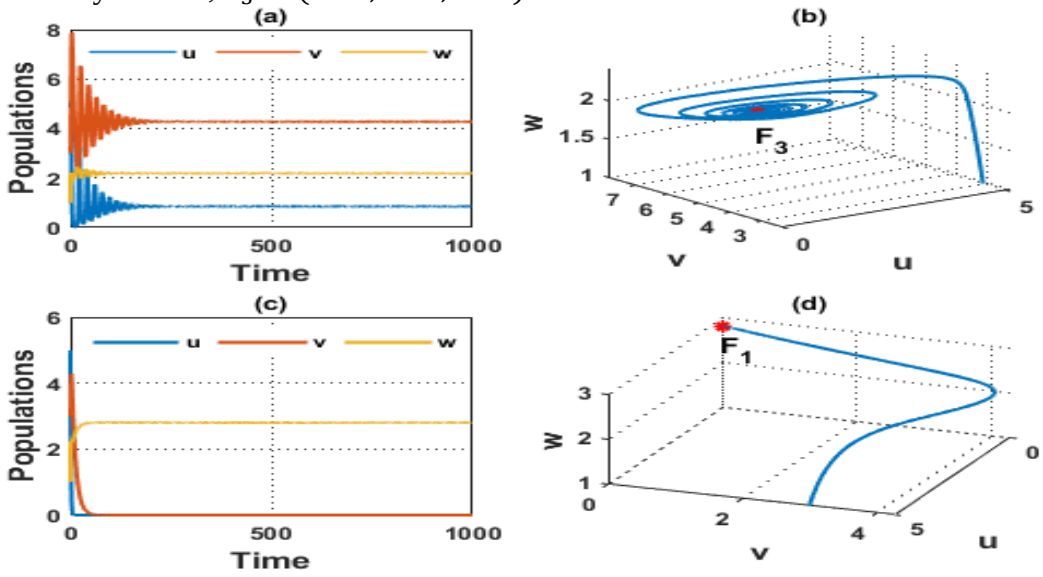


**Figure 3:** Dynamics of the system (1) (a) time series with $r = 0.9$; (b) phase portrait of (a); (c) time series with $r = 0.1$; (d) phase portrait of (c).

Further, Figure (4) investigates the effect of change in the replenishment rate of oxygen in the marine $(s)$ on the stability properties of the system (1). It shows for $s > 0.45$, the solution settles down to CEP. While for $s \leq 0.45$, the solution shows a periodic attractor behaviour.

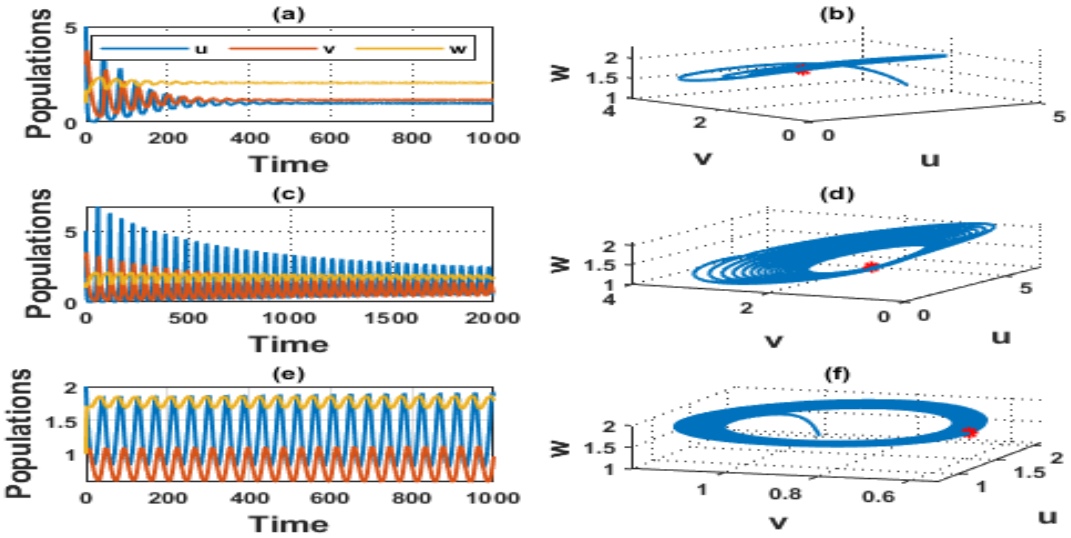


**Figure 4:** Dynamics of system (1) (a) time series with s=0.9; (b) phase portrait of (a); (c) time series with s=0.45; (d) phase portrait of (c); (e) time series with s=0.44; (f) phase portrait of (e).

Now the effect of changing the concentration of dissolved oxygen that comes from several sources $(w_0)$ is explored in Figure (5). The Figure shows that the solution settles asymptotically to the $F_3 = (0.97, 3.36, 1.87)$, for $w_0 > 1.39$. Further, the solution approaches a periodic attractor for $w_0 = 1.39$. While for $w_0 < 1.39$, the solution faces an unstable limit cycle.

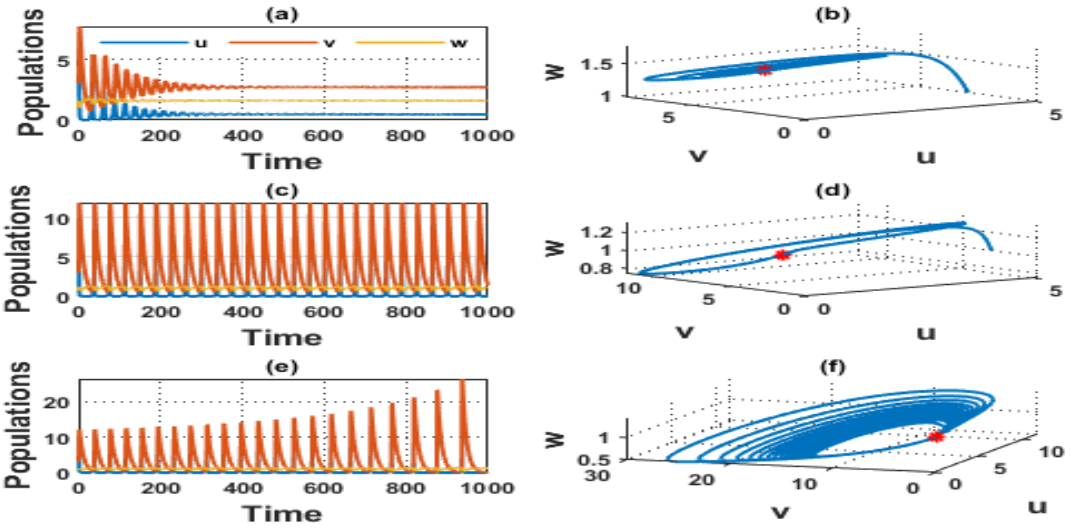


**Figure 5:** Dynamics of system (1) (a) time series with $w_0$ =2; (b) phase portrait of (a); (c) time series with $w_0 = 1.39$; (d) phase portrait of (c); (e) time series with $w_0 = 1.38$; (f) phase portrait of (e).

Next, the influence of changing the amount of oxygen produced by phytoplankton $(d)$ is investigated in Figure (6). The simulation illustrates that for $d \leq 0.77$, the solution stabilizes at its CEP level, while for $d > 0.77$, the solution follows a periodic attractor. The latter result confirms the one obtained in Theorem (2) and Theorem (3), respectively, which establishes the existence of Hopf bifurcation at $d = 0.78$ and the stability of the obtained limit cycle.

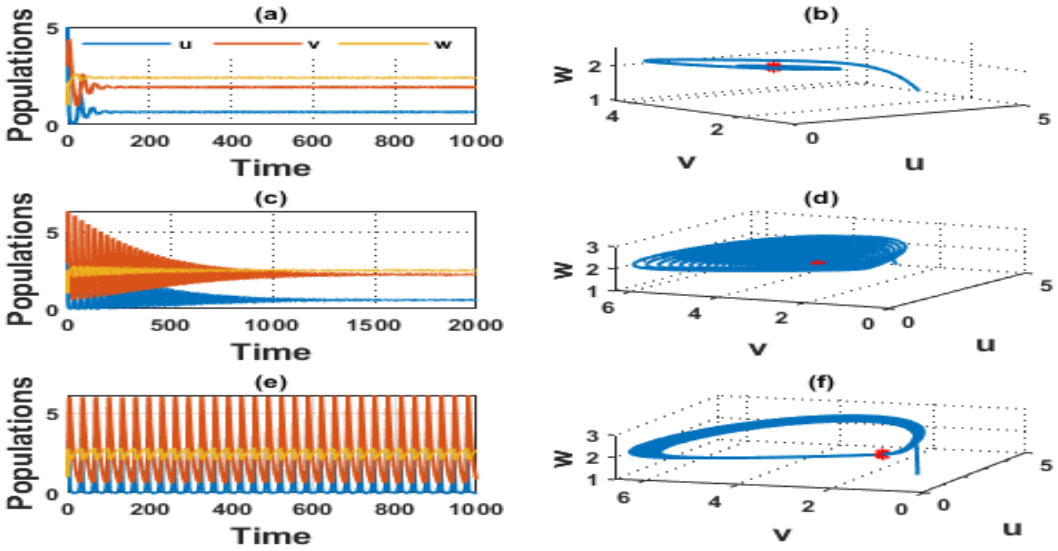


**Figure 6:** Dynamics of system (1) (a) time series with d=0.01; (b) phase portrait of (a); (c) time series with d=0.77; (d) phase portrait of (c); (d) phase portrait of (c); (e) time series with d=0.78; (f) phase portrait of (e).

Finally, for varying the rest parameters given in (15), the solution approaches CEP in the interior of $R_+^3$. For example, Figure (7) shows different values of $\gamma$, and the solution stabilizes at its CEP level.

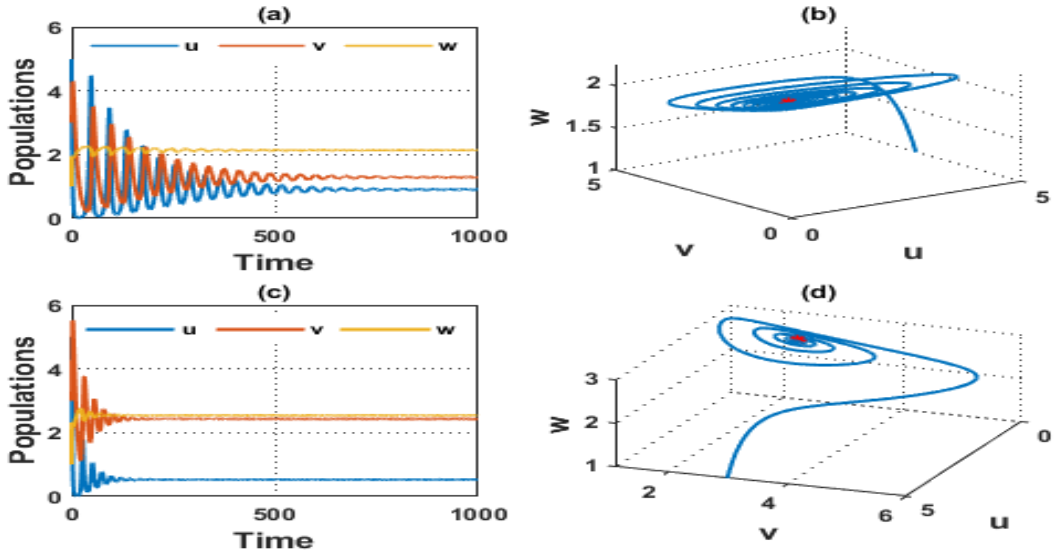


**Figure 7:** Dynamics of system (1) (a) time series with $\gamma = 0.9$; (b) phase portrait of (a); (c) time series with $\gamma = 0.01$; (d) phase portrait of (c).

## 8. Discussions and conclusion

This paper modifies the dissolved oxygen-plankton model by considering that the zooplankton feeds on both available toxic and non-toxic phytoplankton. The idea is to figure out how this kind of interaction affects the dynamics of an aquatic environment. The system underwent theoretical and numerical analysis. The theoretical results detect three steady states; the dissolved oxygen equilibrium point DOEP, the zooplankton-free equilibrium point ZFEP, and CEP. The three steady states show stable or unstable behavior depending on specific conditions. The necessary conditions have been found to ensure the happening of a Hopf bifurcation around CEP.

Nonetheless, the numerical simulation deduced that system (1) always sways about the CEP when the stability criteria are met. Further, by changing the replenishment rate of oxygen in the marine $(s)$, the solution faces extinction for both plankton species or the stability of all components. Moreover, the changing in the value of $w_0, s$ and $d$ leads to the system (1) showing limit cycle behaviour. Finally, the solution is stabilized at the CEP when the remaining parameters are changed. For future work, we suggest considering the impact of climate change on the oxygen-plankton dynamics in the ocean.

**References**

**[1]** V. Hull, L. Parrella, and M. Falcucci, "Modelling dissolved oxygen dynamics in coastal lagoons," *Ecol. Model.*, vol. 211, no. 3–4, pp. 468–480, 2008.

**[2]** A. K. Misra, "Modeling the depletion of dissolved oxygen in a lake due to submerged macrophytes," *Nonlinear Anal. Model. Control*, vol. 15, no. 2, pp. 185–198, 2010.

**[3]** A. K. Misra, P. Chandra, and V. Raghavendra, "Modeling the depletion of dissolved oxygen in a lake due to algal bloom: Effect of time delay," *Adv. Water Resour.*, vol. 34, no. 10, pp. 1232–1238, 2011.

**[4]** Y. Sekerci and S. Petrovskii, "Mathematical modelling of plankton–oxygen dynamics under the climate change," *Bull. Math. Biol.*, vol. 77, no. 12, pp. 2325–2353, 2015.

**[5]** K. Hancke and R. N. Glud, "Temperature effects on respiration and photosynthesis in three diatom-dominated benthic communities," *Aquat. Microb. Ecol.*, vol. 37, no. 3, pp. 265–281, 2004.

**[6]** S. Mandal, S. Ray, and P. B. Ghosh, "Modeling nutrient (dissolved inorganic nitrogen) and plankton dynamics at Sagar island of Hooghly–Matla estuarine system, West Bengal, India," *Nat. Resour. Model.*, vol. 25, no. 4, pp. 629–652, 2012.

**[7]** A. Gökçe, "A mathematical study for chaotic dynamics of dissolved oxygen-phytoplankton interactions under environmental driving factors and time lag," *Chaos, Solitons & Fractals*, vol. 151, p. 111268, 2021.

**[8]** S. Mondal, G. Samanta, and M. De la Sen, "Dynamics of Oxygen-Plankton Model with Variable Zooplankton Search Rate in Deterministic and Fluctuating Environments," *Mathematics*, vol. 10, no. 10, p. 1641, 2022.

**[9]** S. Jawad, D. Sultan, and M. Winter, "The dynamics of a modified Holling-Tanner prey-predator model with wind effect," *Int. J. Nonlinear Anal. Appl.*, vol. 12, no. Special Issue, pp. 2203–2210, 2021.

**[10]** M. Al Nuaimi and S. Jawad, "Modelling and stability analysis of the competitional ecological model with harvesting," *Commun. Math. Biol. Neurosci.*, vol. 2022, p. Article-ID, 2022.

**[11]** S. K. Hassan and S. R. Jawad, "The Effect of Mutual Interaction and Harvesting on Food Chain Model," *Iraqi J. Sci.*, pp. 2641–2649, 2022.

**[12]** S. Jawad, M. Winter, Z.-A. S. A. Rahman, Y. I. A. Al-Yasir, and A. Zeb, "Dynamical Behavior of a Cancer Growth Model with Chemotherapy and Boosting of the Immune System," *Mathematics*, vol. 11, no. 2, p. 406, 2023.

**[13]** S. Dawud and S. Jawad, "Stability analysis of a competitive ecological system in a polluted environment," *Commun. Math. Biol. Neurosci.*, vol. 2022, p. Article-ID, 2022.

**[14]** H. H. Hameed and H. M. Al-Saedi, "Three-Dimensional Nonlinear Integral Operator with the Modelling of Majorant Function," *Baghdad Sci. J.*, vol. 18, no. 2, p. 296, 2021.

**[15]** A. M. Kareem and S. N. Al-Azzawi, "A stochastic differential equations model for the spread of coronavirus COVID-19): the case of Iraq," *Iraqi J. Sci.*, pp. 1025–1035, 2021.

**[16]** Sajan, S. K. Sasmal, and B. Dubey, "A phytoplankton–zooplankton–fish model with chaos control: In the presence of fear effect and an additional food," *Chaos An Interdiscip. J. Nonlinear Sci.*, vol. 32, no. 1, p. 13114, 2022.

**[17]** X.-Y. Meng and L. Xiao, "Stability and Bifurcation for a Delayed Diffusive Two-Zooplankton One-Phytoplankton Model with Two Different Functions," *Complexity*, vol. 2021, 2021.

**[18]** T. G. Hallam, C. E. Clark, and G. S. Jordan, "Effects of toxicants on populations: a qualitative approach II. First order kinetics," *J. Math. Biol.*, vol. 18, no. 1, pp. 25–37, 1983.

**[19]** S. Chakraborty, S. Chatterjee, E. Venturino, and J. Chattopadhyay, "Recurring plankton bloom dynamics modeled via toxin-producing phytoplankton," *J. Biol. Phys.*, vol. 33, no. 4, pp. 271–290, 2007.
**[20]** J. Dhar and R. S. Baghel, "Role of dissolved oxygen on the plankton dynamics in spatio-temporal domain," *model. Earth Syst. Environ.*, vol. 2, no. 1, pp. 1–15, 2016.
**[21]** M. W. Hirsch, S. Smale, and R. L. Devaney, *Differential equations, dynamical systems, and an introduction to chaos*. Academic press, 2012.
**[22]** L. Perko, *Differential equations and dynamical systems*, vol. 7. Springer Science & Business Media, 2013.
**[23]** J. P. LaSalle, "Stability theory and invariance principles," in *Dynamical systems*, Elsevier, 1976, pp. 211–222.
**[24]** R. M. May, *Stability and complexity in model ecosystems*. Princeton university press, 2019.
**[25]** S. R. Jawad and M. Al Nuaimi, "Persistence and bifurcation analysis among four species interactions with the influence of competition, predation and harvesting," *Iraqi J. Sci.*, pp. 1369–1390, 2023.
**[26]** D. Mukherjee, "Study of fear mechanism in predator-prey system in the presence of competitor for the prey," *Ecol. Genet. Genomics*, vol. 15, p. 100052, 2020.